Pure and conformal CVD nickel and nickel monosilicide in high-aspect-ratio structures analyzed by atom probe tomography

Kecheng Li, Jun Feng, Junkeun Kwak, Jing Yang, and Roy G. Gordon

Citation: Journal of Applied Physics **121**, 175301 (2017); doi: 10.1063/1.4982670
View online: http://dx.doi.org/10.1063/1.4982670
View Table of Contents: http://aip.scitation.org/toc/jap/121/17
Published by the American Institute of Physics

Pure and conformal CVD nickel and nickel monosilicide in high-aspect-ratio structures analyzed by atom probe tomography

Kecheng Li,[1] Jun Feng,[2] Junkeun Kwak,[3] Jing Yang,[1] and Roy G. Gordon[1,2,a)]
[1]*John A. Paulson School of Engineering and Applied Sciences, Harvard University, Cambridge, Massachusetts 02138, USA*
[2]*Department of Chemistry and Chemical Biology, Harvard University, Cambridge, Massachusetts 02138, USA*
[3]*Samsung Electronics Co., Ltd., Nongseo-Dong, Giheung-Gu, Yongin-city, Gyeonggi-Do 446-711, South Korea*

(Received 1 February 2017; accepted 15 April 2017; published online 2 May 2017)

Low-resistance and uniform contacts are needed for modern 3-D silicon transistors. The formation of high-quality and conformal nickel silicide at the interface between silicon and metal contacts is a possible solution. Direct-liquid-evaporation chemical vapor deposition is used to deposit nickel films conformally inside narrow silicon trenches. The deposited Ni is then reacted with a silicon substrate to form nickel monosilicide. Atom probe tomography (APT) is used to find and count the atoms in nanoscale regions inside these 3-D structures. APT shows that these NiSi films are stoichiometrically pure, single-phase, and conformal even inside trenches with high aspect ratios. The APT technique measures all impurities, including carbon, nitrogen, and oxygen, to have concentrations less than 0.1 at. %. *Published by AIP Publishing*. [http://dx.doi.org/10.1063/1.4982670]

I. INTRODUCTION

As the miniaturization process of modern electronics continues, interfaces become critical for the overall performance and durability of electronic devices. One of the most important interfacial properties is the contact resistance between silicon and metals.[1–3] Ni, Co, and Ti are usually considered favorable contact metals for silicon because they all react with silicon to form stable silicides with low contact resistance.[4,5] In advanced semiconductor manufacturing processes, the formation of nickel silicide is emerging as the preferred contact with silicon due to its lower formation temperature, lower resistance, and smoother interface than Co and Ti silicides.[6] Nickel monosilicide (NiSi) also consumes less silicon during silicide formation than $CoSi_2$ or $TiSi_2$, the phases commonly formed by Co and Ti. NiSi has a low resistivity of around 14 mΩ cm and only requires formation temperature below 400 °C, whereas $NiSi_2$ forms only above 600 °C and Ni_2Si is unstable when interfacing with silicon.[7,8] Therefore, to enable higher-performance silicon devices, a process is needed for making high-quality NiSi at Ni/Si interfaces inside 3-D structures.

In modern ultra-large-scale integrated (ULSI) architectures, blocks with different functionalities are connected three-dimensionally. Thus, semiconductor devices and interconnects must be made inside structures with high aspect ratios.[9,10] For example, fin-type field-effect transistors (Fin-FETs) with high-aspect-ratio silicon fins need conformal coating of dielectrics, amorphous silicon (a-Si) gates, and the metal/silicide (e.g., Ni/NiSi) contacting a-Si gates, as illustrated in Figure 1(a). Also, in multi-layer electronics, long through-silicon vias (TSVs) with ultra-small diameters are necessary to form contact with silicon devices on the substrate, which requires the formation of NiSi inside deep holes (Figure 1(b)).[11] Great difficulties have been encountered by the industry in depositing conformal metal films inside high-aspect-ratio structures due to the anisotropic nature of available physical vapor deposition techniques.[12] To overcome this difficulty, direct-liquid-evaporation

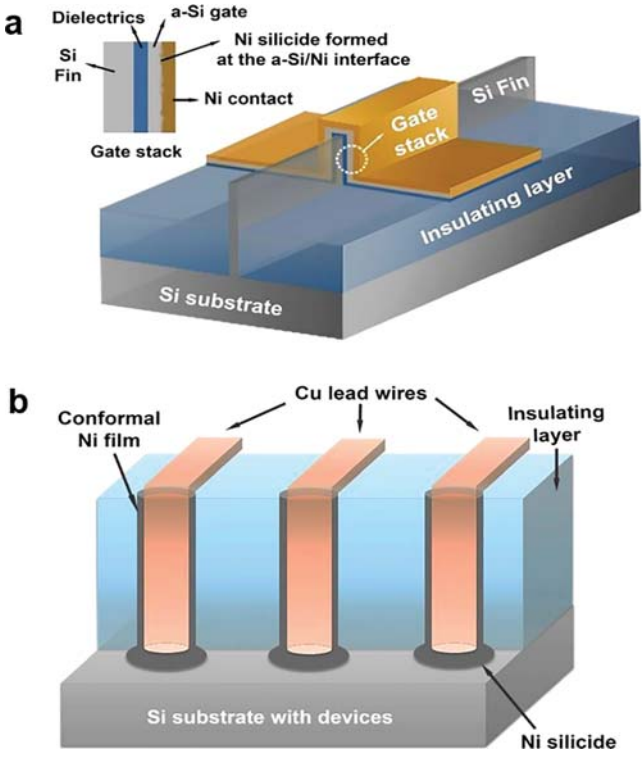

FIG. 1. (a) Schematic illustration of Ni silicide applied on Fin-FETs, improving the contact between a-Si gates and lead wires. (b) Formation of Ni silicide deep inside hole structures facilitates the contact between copper TSVs and silicon substrates with devices.

a)Author to whom correspondence should be addressed. Electronic mail: gordon@chemistry.harvard.edu

chemical vapor deposition (DLE-CVD) of Ni, which can be readily transformed into NiSi at its interface with silicon, has been introduced in recent research reports.[13,14]

In contrast to conventional CVD with bubbler sources of vapor, liquid precursor solutions in DLE-CVD systems are stored unheated and directly injected into the heated evaporation region. The DLE process heats a precursor only very briefly, thereby avoiding decomposition that can occur when a conventional bubbler is heated for a long time. DLE provides a higher vapor pressure of precursors, which is needed to deposit highly conformal CVD films inside high-aspect-ratio features.[15] Moreover, the precursor delivery rate of DLE-CVD is controlled by the very stable injection rate of a liquid precursor or a precursor solution, instead of the variable precursor vapor pressure found in conventional bubblers.[16] These features of DLE-CVD enable the formation of films with much higher conformality and better reproducibility.

DLE-CVD provides highly conformal coatings of Ni thin films and thus conformal NiSi layers; however, the reported compositional and structural characterizations of these materials have been mostly conducted on planar samples rather than directly on the specimens deep inside high-aspect-ratio structures.[17] Due to different vapor concentrations during CVD of a film inside and outside of a high-aspect-ratio structure, it is possible that some properties of the material deposited outside will differ from the material deposited inside.[18] To test this possibility, a method is needed to analyze materials from both outside and inside narrow structures. Atom probe tomography (APT) is an advanced characterization method with atomic resolution from both compositional and morphological points of view.[19,20] With focused ion beam (FIB) sample preparation techniques, specimens from deep inside high-aspect-ratio structures can be physically lifted-out and sharpened into ultrasmall needles (~30 nm tip diameter) suitable for APT analysis.[21]

In this report, we demonstrate by APT analysis that high-purity NiSi can be formed by annealing Ni films deposited by DLE-CVD inside narrow silicon trench structures. By optimizing the DLE-CVD Ni deposition conditions, we produced Ni films with ~4% N as an active component in order to form smooth Si/NiSi interfaces.[22] Highly uniform Ni and Si distributions in specimens from both outside and inside of trenches are demonstrated with close to stoichiometric 1:1 Ni-to-Si atomic ratios. All impurities found in the NiSi are less than 0.1 atomic per cent. This work provides evidence that DLE-CVD of Ni is a promising approach to the fabrication of uniform contacts with silicon inside high-aspect-ratio structures, thus contributing to the further miniaturization of semiconductor devices.

II. EXPERIMENTAL DETAILS

The precursor used in this work is nickel(II) bis(*N*,*N*′-*tert*-butylacetamidinate), $Ni(MeC(N^tBu)_2)_2$, (Figure S1 in the supplementary material), which was synthesized by a previously reported method.[13,14] Tetradecane (Aldrich Chemical Co.) was dried by distilling from sodium inside a Schlenk line setup. All other solvent and precursor manipulations were conducted in a glove box under a nitrogen atmosphere. Before depositions, all Si samples were cleaned with acetone and isopropanol and finally dipped in the 5% aqueous HF solution for about 10 s to remove the native oxide layer.

The CVD of Ni was conducted with a home-made direct liquid evaporation (DLE) system (Figure S2). In brief, the $Ni(MeC(N^tBu)_2)_2$ precursor solution (20 wt. % in tetradecane) was injected by using a syringe pump at a rate of 0.1 mL/min into a heated vaporization tube inside an oven that was heated to 150 °C. During the vaporization, the precursor vapor was mixed with 60 cubic centimeters per minute (sccm) purified nitrogen and then introduced into a deposition chamber preheated to 160 °C. As co-reactants, the 60 sccm total flow of a mixture of hydrogen and ammonia was diluted with 60 sccm of N_2 and introduced into the deposition chamber along with the nickel precursor vapor mixture. Using a pressure controller, the total pressure in the reactor chamber was regulated at 10 Torr, which was then maintained throughout the deposition process. Inside the reaction chamber, an aluminum half-cylinder was used as the sample holder, in which a resistive heater and a thermocouple were embedded to elevate slightly the holder temperature to be about 10 °C above the chamber wall. After deposition of Ni, the sample was then heated to 470 °C under 1 Torr of flowing nitrogen for 3 min, without an air break, to form Ni silicide at the Si-Ni interface.[14]

Trench samples with 10:1 aspect ratio test structures were fabricated by the Bosch-type deep silicon reactive ion etching (DRIE) process with SF_6 and C_4F_6 gases.[23] In the fabrication process, 1 μm of ZEP-A e-beam resist patterned by e-beam lithography was used as the soft mask.

APT specimens from both outside and deep inside the trench were acquired with a dual-beam focused ion beam (FIB) system. Specimens were collected along directions parallel to the sample surfaces, followed by annular milling with a Ga^+ ion beam to sharpen the specimens into needles with radii between 20 nm and 50 nm and with a shank angle around 10°.[24] The analyses were carried out at a temperature of 50 K under a vacuum pressure lower than 5×10^{-11} Torr. A 532 nm laser was used to assist ion evaporation. Its energy was set to be 50 pJ/pulse, and the pulse frequency was set to be 100 kHz. The average evaporation rate was maintained at 0.5 ion per pulse. Data reconstruction was performed with IVAS software (Cameca, Gennevilliers, France) incorporating standard reconstruction algorithms, enabling the extraction of three-dimensional quantitative compositional and structural information.[25] The data analysis process decomposes complex ions such as SiO^+ and NiH^+ into single atoms and differentiates overlapped peaks such as $^{28}Si^{2+}$ and $^{14}N^+$ by using the abundance ratios among different isotopes. This analysis process can only be computed with an adequate amount of statistical data; in this regard, the trace amount of N was only observed in the larger analyzed regions but not in the 1D compositional depth profile since the 1D profile is based on thin slices with too few data points.

The cross-sectional morphology of thin films was visualized on the Zeiss Ultra55 field-emission scanning electron microscope (FE-SEM), from which the thickness of each

film was measured. The depth-profile elemental analysis was carried out by X-ray photoelectron spectroscopy (XPS). The surface roughness of the films was analyzed by atomic force microscopy (AFM) (Asylum Model MFP-3D AFM system). The Cameca LEAP 4000X HR system was used for APT analysis.

III. RESULTS AND DISCUSSION

Figure 2(a) show a plot of the growth rate and the N/Ni ratio of the as-deposited film versus the NH_3 percentage in the co-reactants (60 sccm total flow of H_2 plus NH_3) used in DLE-CVD. The results show that a lower NH_3 percentage generally leads to a lower nitrogen content; however, when the NH_3 percentage approaches 0%, the growth rate decreases toward 0. NH_3 is apparently needed to chemisorb the Ni precursor onto the surface of the growing film. For the conversion from Ni to NiSi, low impurity content is required in order to obtain high-purity NiSi and also to minimize structural changes during silicidation. Nevertheless, pure nickel with zero nitrogen content is not desirable because different thicknesses of NiSi then form on different crystal planes of silicon due to different diffusion rates of Ni in different directions through Si.[26] Thus, a small, but non-zero, nitrogen content in the nickel is needed to slow down the out-diffusion of nickel, thereby producing a uniform silicide thickness on all crystallographic orientations of the silicon.[27] To achieve a suitable growth rate and a relatively low N content in Ni films, 50 sccm H_2 with 10 sccm NH_3 (16.7% NH_3) was adopted as the recipe for Ni deposition used in this work. An AFM image of the smooth morphology of the Ni film is shown in Figure 2(b), giving an average RMS surface roughness value of 3.5 nm, which is only 1.3% of the 262 nm thickness.

As a platform to demonstrate conformality of DLE-CVD-Ni and its conversion to NiSi in structures with high aspect ratios, silicon trenches with an aspect ratio of 10:1 were fabricated as test structures by a Bosch-type DRIE process. Figure 2(c) shows a cross-sectional SEM image of the resulting trench, the width and depth of which are 0.7 μm and 7 μm, respectively. After 90 min of the Ni DLE-CVD process, a highly conformal Ni coating is observed in the trench (Figure 2(d)). The thickness is 262 nm both inside and outside of the trench, indicating that the Ni DLE-CVD process is capable of coating the test structure with extremely high uniformity and conformality. It should be noted that the aspect ratio of trenches increases from 10:1 up to 40:1 near the end of the deposition since the Ni coating reduces the width without decreasing the depth of the trench very much. Afterwards, the Ni-coated trench sample was annealed in N_2 at 470 °C for 3 min, during which NiSi was formed at the interface between the Ni and the Si substrate. Based on the cross-sectional SEM image shown in Figure 3(a), approximately 160 nm of NiSi formed at the interface, leaving about 100 nm of unreacted Ni on top of the NiSi.

The FIB sample preparation process is illustrated in Figures 3(a)–3(f). First, a region containing one entire side of a trench, indicated by the white dashed box in Figures 3(a) and 3(b), was extracted and mounted on a flat-top silicon post (Figure 3(c)). The upper side of the piece (referred as "outside specimen") was aligned with the center of the post and welded onto it by *in-situ* FIB deposition of tungsten. Then, another part of the piece was cut and mounted onto another post, becoming the "inside specimen" (Figure 3(d)). Afterwards, these specimens were cut into a pyramid shape (Figure 3(e)) and further sharpened into ultra-small needles (Figure 3(f)) by annular milling.

Two APT analysis results from the "outside specimen" and "inside specimen" are shown in Figures 4(a)–4(f). The analysis lengths of the outside and inside specimens are 200 nm and 360 nm presented in Figures 4(a) and 4(d), respectively. The large volume ($40 \times 30 \times 200\,nm^3$ and $50 \times 30 \times 360\,nm^3$) of analyzed atoms guarantees that reliable statistical information can be obtained from one dataset. The spacial distribution of Ni and Si atoms is shown in Figures 4(b), 4(e), 4(c), and 4(f). Ni and Si atoms are

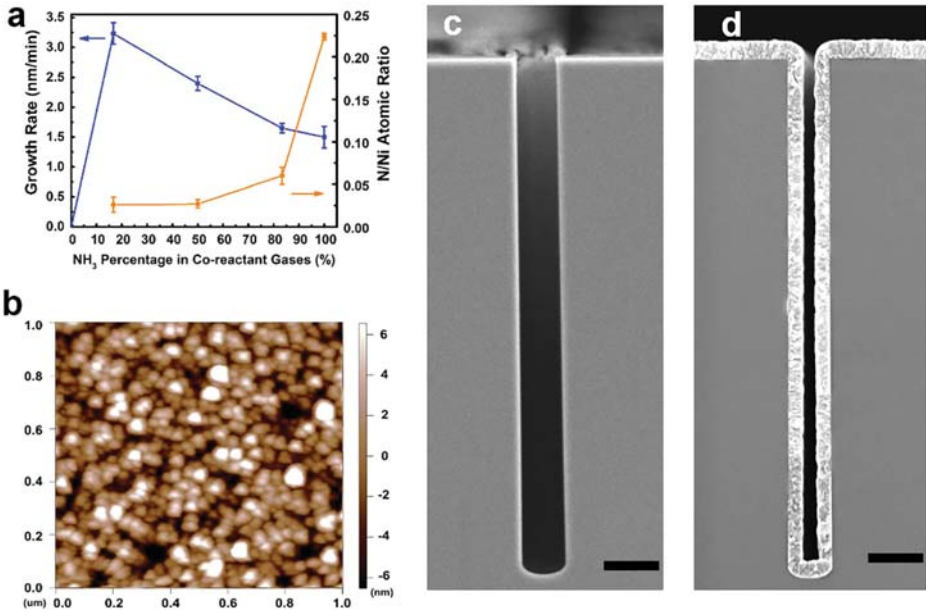

FIG. 2. (a) Growth rate and N/Ni atomic ratio plotted versus the NH3 percentage out of the NH3/H2 co-reactant mixture (60 sccm in total) used during the DLE-CVD process. (b) Taping-mode AFM image on the surface of the Ni film. (c) Cross-sectional SEM images of a silicon trench test structure. (d) The same silicon trench after Ni deposition, demonstrating the conformality of the deposited film.

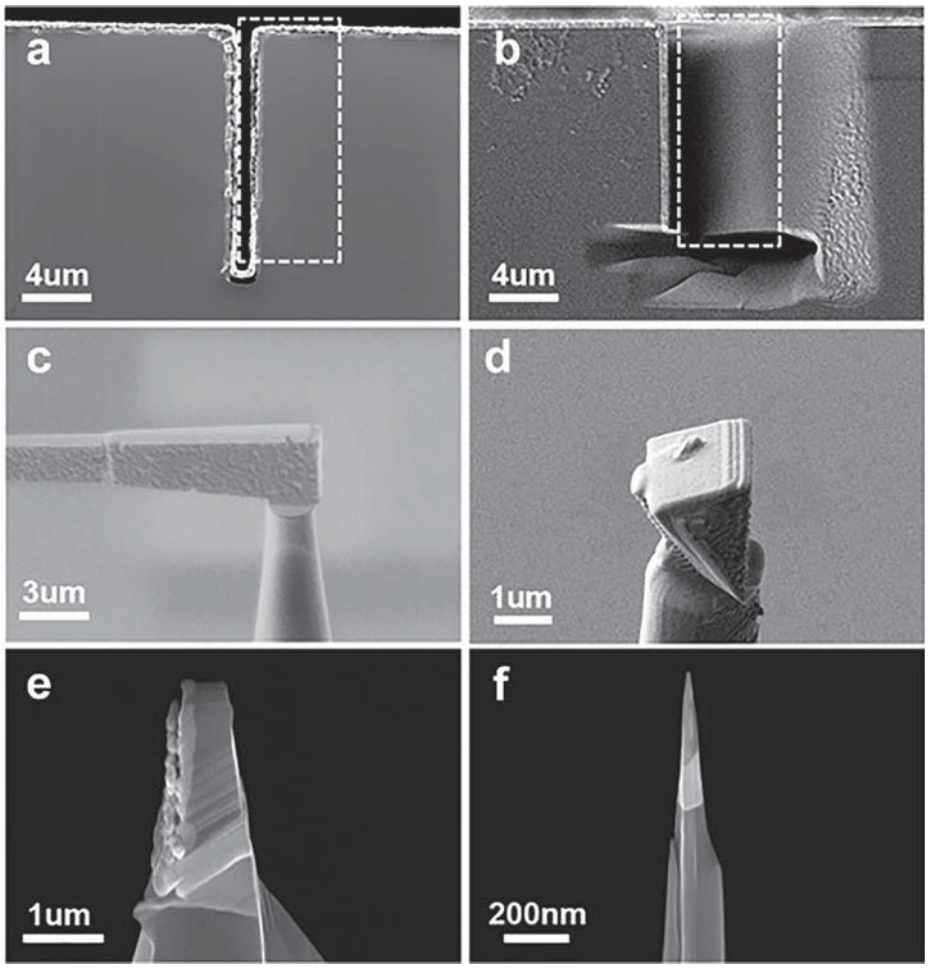

FIG. 3. Atom probe sample preparation process by the focused ion beam (FIB) lift-off technique. (a) Cross-sectional SEM image of the Ni silicide sample with a white dashed box indicating the lift-out target region. (b) SEM image of the same area shown in (a) after lifting out the target region. (c) The lifted-out specimen welded onto a silicon needle by tungsten metal deposition by FIB. (d) The specimen after cutting off the redundant part. (e) The specimen was further cut to make a tapered shape. (f) The final needle-shaped specimen for atom probe analysis after annular milling.

represented as blue and grey dots, respectively. The distribution of Ni and Si atoms is highly uniform with no observable phase separation or clustering phenomenon.

Based on the mass spectra (Figures S3 and S4 in the supplementary material), compositional information was obtained from 10 nm diameter cylindrical regions perpendicular to the Ni silicide interfaces in the specimens from both inside and outside the trench. To avoid analyzing the top surface region, which was potentially contaminated or damaged during the sample preparation processes, ~60 nm layers on the top surfaces of the specimens were electrically evaporated before recording APT data, thus exposing the pristine bulk samples for analysis. Data processing with IVAS software (Cameca, Gennevilliers, France) determined the compositions of the analyzed regions inside and outside the trench (Table I). Nearly equal concentrations of Ni and Si (about 50% each) are observed, and the distributions of Ni and Si are uniform, as shown in Figure 4. We thus conclude that the analyzed specimen is a single-phase of NiSi, rather than a mixture of different phases such as Ni_2Si and $NiSi_2$.

Aside from Ni and Si, only less than 0.1% of O, N, and C impurities were detected in the NiSi phase, which shows its ultrahigh purity. Also, the composition of the DLE-CVD Ni is shown in Table II, which demonstrates a Ni film including ~4% nitrogen. This N content makes the Si/NiSi interface smooth. Pure nickel without this nitrogen content would have produced nickel silicide with different thicknesses on different silicon orientations.[27] Compared with the composition of the as-deposited Ni film, the N, O, and C impurity levels dramatically decreased after the silicidation process. These impurities did not diffuse into the silicon along with nickel, and thus, they remain in the unreacted nickel, which will be eventually etched away from the surface. We note that these ultra-low concentrations of impurities in the NiSi are undetectable by most conventional elemental analysis methods, including XPS, RBS, EDX, XRF, and EELS. Therefore, APT analysis can measure quantitatively and visualize the positions of trace amounts of impurities, enabling fine adjustments and improvements to modern functional materials for the semiconductor industry.

IV. CONCLUSIONS

We obtained quantitative composition and elemental distribution of NiSi converted from DLE-CVD-deposited Ni, using FIB lift-off and APT analysis techniques. Because of the high conformality of the DLE-CVD process, the same composition and uniformity were found in the Ni and NiSi specimens from both inside and outside of high-aspect-ratio trenches. APT demonstrated a nearly 1:1 Ni-to-Si atomic ratio and highly uniform distributions of both Ni and Si, proving the formation of single-phase NiSi. APT located and

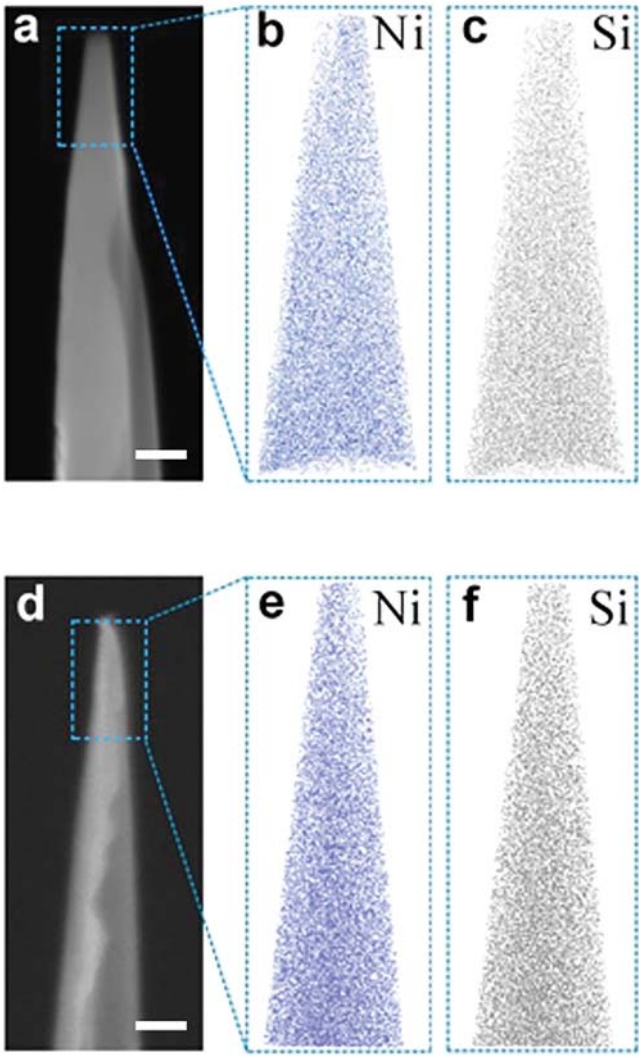

FIG. 4. Ni and Si elemental atom probe reconstruction images of the specimens from outside ((b) and (c)) and deep inside ((e) and (f)) of a trench, corresponding to the SEM images shown in (a) and (b), respectively. The scale bar is 100 nm.

quantified the trace amounts of C, N, and O impurities (<0.1 at. %), which are undetectable by most analytical methods. These results demonstrate that DLE-CVD of Ni and its conversion to pure and highly conformal NiSi is a promising approach for the semiconductor industry to make 3-D contacts to silicon. APT showed an outstanding capability to reveal low concentrations of impurities and their uniform spatial distribution on a nanometer scale. This highly detailed information offers important feedback for the application of better functional materials in future advanced electronic devices.

TABLE I. Atom probe analyses of NiSi specimens obtained from both inside and outside of the trench structure. Atomic percentage errors were estimated by doing multiple runs of peak identification, fitting, and decomposition using the IVAS software.

Element	Outside trench Atomic percentage (%)	Inside trench Atomic percentage (%)
Ni	52.00 ± 0.03	50.12 ± 0.05
Si	47.87 ± 0.10	49.83 ± 0.09
C	0.02 ± 0.01	0.005 ± 0.004
N	0.04 ± 0.02	0.03 ± 0.02
O	0.07 ± 0.03	0.015 ± 0.005

TABLE II. Atom probe analyses of as-deposited nickel nitride specimens obtained from both inside and outside of the trench structure.

Element	Outside trench Atomic percentage (%)	Inside trench Atomic percentage (%)
Ni	93.42 ± 0.10	94.98 ± 0.10
Si	Not detected	Not detected
C	1.52 ± 0.15	0.95 ± 0.20
N	4.09 ± 0.10	3.66 ± 0.09
O	0.97 ± 0.30	0.41 ± 0.20

SUPPLEMENTARY MATERIAL

See supplementary material for further description of the DLE-CVD system, Co precursor, and additional atom probe analysis results.

ACKNOWLEDGMENTS

We acknowledge financial support from the Samsung Electronics Co., Ltd., under Contract No. SLSI-201304DD044. We thank Dr. Andrew Magyar, senior imaging scientist at the Center for Nanoscale Systems of Harvard University, for help with APT sample preparation, measurements, data analysis, and discussions.

[1]F. Leonard and A. A. Talin, Nat. Nanotechnol. **6**, 773 (2011).
[2]H. Iwai, Microelectron. Eng. **86**, 1520 (2009).
[3]A. Chaudhry, V. Ramamurthi, E. Fong, and M. S. Islam, Nano Lett. **7**, 1536 (2007).
[4]A. E. Morgan, E. K. Broadbent, M. Delfino, B. Coulman, and D. K. Sadana, J. Electrochem. Soc. **134**, 925 (1987).
[5]Y. Wu, J. Xiang, C. Yang, W. Lu, and C. M. Lieber, Nature **430**, 61 (2004).
[6]H. Iwai, T. Ohguro, and S.-I. Ohmi, Microelectron. Eng. **60**, 157 (2002).
[7]M. K. Datta, S. K. Pabi, and B. S. Murty, Mater. Sci. Eng. A **284**, 219 (2000).
[8]D. Mangelinck, K. Hoummada, F. Panciera, M. El Kousseifi, I. Blum, M. Descoins, M. Bertoglio, A. Portavoce, C. Perrin, and M. Putero, Phys. Status Solidi A **211**, 152 (2014).
[9]R. Chau, B. Doyle, S. Datta, J. Kavalieros, and K. Zhang, Nat. Mater. **6**, 810 (2007).
[10]A. Franco, J. Geissbuhler, N. Wyrsch, and C. Ballif, Sci. Rep. **4**, 4597 (2014).
[11]C. Lavoie, F. M. d'Heurle, C. Detavernier, and C. Cabral, Jr., Microelectron. Eng. **70**, 144 (2003).
[12]Y. Au, Q. M. Wang, H. Li, J.-S. M. Lehn, D. V. Shenai, and R. G. Gordon, J. Electrochem. Soc. **159**, D382 (2012).
[13]Z. Li, R. G. Gordon, V. Pallem, H. Li, and D. V. Shenai, Chem. Mater. **22**, 3060 (2010).
[14]Z. Li, R. G. Gordon, H. Li, D. V. Shenai, and C. Lavoie, J. Electrochem. Soc. **157**, H679 (2010).
[15]J. Yang, K. Li, J. Feng, and R. G. Gordon, J. Mater. Chem. C **3**, 12098 (2015).
[16]J.-H. Lee and S.-W. Rhee, J. Mater. Res. **14**, 3988 (1999).
[17]K. Shuichi, H. Yukinori, O. Yoshifumi, Y. Tadashi, K. Keiichiro, M. Naofumi, K. Toshiharu, H. Nobuyoshi, K. Toru, and N. Koji, Jpn. J. Appl. Phys., Part 1 **53**, 021301 (2014).
[18]W. B. Wang, N. N. Chang, T. A. Codding, G. S. Girolami, and J. R. Abelson, J. Vac. Sci. Technol. A **32**, 051512 (2014).
[19]D. Blavette, A. Bostel, J. M. Sarrau, B. Deconihout, and A. Menand, Nature **363**, 432 (1993).

[20]B. Gault, M. P. Moody, J. M. Cairney, and S. P. Ringer, Mater. Today **15**, 378 (2012).
[21]F. Panciera, K. Hoummada, M. Gregoire, M. Juhel, F. Lorut, N. Bicais, and D. Mangelinck, Microelectron. Eng. **107**, 167 (2013).
[22]A. Alberti, C. Bongiorno, C. Spinella, and A. L. Magna, Phys. Status Solidi C **11**, 164 (2014).
[23]P. Kim, W. E. Adorno-Martinez, M. Khan, and J. Aizenberg, Nat. Protocols **7**, 311 (2012).
[24]K. Hono, D. Raabe, S. P. Ringer, and D. N. Seidman, MRS Bull. **41**, 23 (2016).
[25]M. Knop, P. Mulvey, F. Ismail, A. Radecka, K. M. Rahman, T. C. Lindley, B. A. Shollock, M. C. Hardy, M. P. Moody, T. L. Martin, P. A. J. Bagot, and D. Dye, J. Miner. Met. Mater. Soc. **66**, 2495 (2014).
[26]J. O. Olowolafe, M. A. Nicolet, and J. W. Mayer, Thin Solid Films **38**, 143 (1976).
[27]A. R. Zanatta, D. C. Ingram, and M. E. Kordesch, J. Appl. Phys. **116**, 123508 (2014).